ORIGINAL RESEARCH

Lysophosphatidic Acid Signaling through the Lysophosphatidic Acid-1 Receptor Is Required for Alveolarization

Manuela Funke[1,2,3*], Lars Knudsen[4*], David Lagares[3], Simone Ebener[1,2], Clemens K. Probst[3], Benjamin A. Fontaine[3], Alicia Franklin[3], Manuela Kellner[4], Mark Kühnel[4], Stephanie Matthieu[4], Roman Grothausmann[4], Jerold Chun[5], Jesse D. Roberts Jr.[6], Matthias Ochs[4] , and Andrew M. Tager[3]

[1]Departments of Pulmonary Medicine, Inselspital Berne, and [2]Clinical Research, University of Berne, Berne, Switzerland; [3]Division of Pulmonary and Critical Care Medicine and Center for Immunology and Inflammatory Diseases, and [6]Cardiovascular Research Center, Massachusetts General Hospital, Harvard Medical School, Boston, Massachusetts; [4]Institute of Functional and Applied Anatomy, Hannover Medical School, and Biomedical Research in Endstage and Obstructive Lung Disease Hannover (BREATH), German Center for Lung Research, REBIRTH Cluster of Excellence, Hannover, Germany; and [5]Department of Molecular and Cellular Neuroscience, Dorris Neuroscience Center, Scripps Research Institute, La Jolla, California

Abstract

Lysophosphatidic acid (LPA) signaling through one of its receptors, LPA_1, contributes to both the development and the pathological remodeling after injury of many organs. Because we found previously that LPA–LPA_1 signaling contributes to pulmonary fibrosis, here we investigated whether this pathway is also involved in lung development. Quantitative assessment of lung architecture of LPA_1-deficient knockout (KO) and wild-type (WT) mice at 3, 12, and 24 weeks of age using design-based stereology suggested the presence of an alveolarization defect in LPA_1 KO mice at 3 weeks, which persisted as alveolar numbers increased in WT mice into adulthood. Across the ages examined, the lungs of LPA_1 KO mice exhibited decreased alveolar numbers, septal tissue volumes, and surface areas, and increased volumes of the distal airspaces. Elastic fibers, critical to the development of alveolar septa, appeared less organized and condensed and more discontinuous in KO alveoli starting at P4. Tropoelastin messenger RNA expression was decreased in KO lungs, whereas expression of matrix metalloproteinases degrading elastic fibers was either decreased or unchanged. These results are consistent with the abnormal lung phenotype of LPA_1 KO mice, being attributable to reduced alveolar septal formation during development, rather than to increased septal destruction as occurs in the emphysema of chronic obstructive pulmonary disease. Peripheral septal fibroblasts and myofibroblasts, which direct septation in late alveolarization, demonstrated reduced production of tropoelastin and matrix metalloproteinases, and diminished LPA-induced migration, when isolated from LPA_1 KO mice. Taken together, our data suggest that LPA–LPA_1 signaling is critically required for septation during alveolarization.

Keywords: alveolarization; lung development; LPA_1; elastin; matrix metalloproteinase

Clinical Relevance

The molecular pathways driving the developmental processes involved in alveolarization remain to be fully elucidated. Here we describe a critical role for lysophosphatidic acid (LPA) signaling through the LPA_1 receptor in alveolar septation. In contrast to previous studies in pulmonary fibrosis, which have indicated that antagonizing LPA–LPA_1 signaling may be able to mitigate that pathology, the current study suggests that augmenting LPA–LPA_1 signaling may have the potential to contribute to future strategies to stimulate alveolar septation when that may be beneficial.

(Received in original form May 7, 2015; accepted in final form January 4, 2016)

*These authors contributed equally to this article.

This work was supported by National Institutes of Health grants R01HL095732 and R01HL108975 (A.M.T.), R01HL125715 (J.D.R.), and R01NS084398 (J.C.).

Author Contributions: Conception and design: M.F., L.K., J.D.R., and A.M.T.; data acquisition: M.F., L.K., D.L., S.E., C.K.P., B.A.F., A.F., M. Kellner, M. Kühnel, S.M., R.G., and J.D.R.; analysis and interpretation: M.F., L.K., D.L., S.E., M. Kellner, M. Kühnel, S.M., R.G., J.D.R., and A.M.T.; drafting the manuscript: M.F. and A.M.T.; revising the manuscript for important intellectual content: M.F., L.K., D.L., S.E., C.K.P., B.A.F., M. Kellner, M. Kühnel, S.M., R.G., J.C., J.D.R., M.O., and A.M.T.

Correspondence and requests for reprints should be addressed to Manuela Funke, M.D., Department of Pulmonary Medicine, Inselspital, University Hospital, Berne, 3010 Berne, Switzerland. E-mail: manuela.funke-chambour@insel.ch

This article has an online supplement, which is accessible from this issue's table of contents at www.atsjournals.org

Am J Respir Cell Mol Biol Vol 55, Iss 1, pp 105–116, Jul 2016
Copyright © 2016 by the American Thoracic Society
Originally Published in Press as DOI: 10.1165/rcmb.2015-0152OC on January 21, 2016
Internet address: www.atsjournals.org

Lysophosphatidic acid (LPA) is a bioactive lipid mediator that directs multiple fundamental biological processes, including those that regulate cell fate, such as survival, proliferation and apoptosis, and those that regulate cell motility, such as extension and contraction of the actin cytoskeleton (1–3). The effects of LPA on cells depend on their expression of LPA-specific G-protein coupled receptors (e.g., LPA_{1-6} [1, 4]). Moreover, different downstream signaling pathways couple to each LPA receptor, enabling the same LPA receptor to mediate opposing effects in different cells types (5). Dysregulation of LPA signaling specifically through LPA_1 has been found to produce anatomic and functional defects in developing animals and to contribute to disease pathology in adult animals in multiple different organ systems (1). Previously, we linked the LPA–LPA_1 pathway to the development of pulmonary fibrosis, through its ability to promote epithelial cell apoptosis, vascular leak, and fibroblast migration and resistance to apoptosis (5, 6). Aberrant reactivation of developmental pathways is characteristic of malignant diseases and may also be characteristic of diseases of pathological tissue remodeling, such as pulmonary fibrosis (7). Given the important roles that we have identified for LPA–LPA_1 signaling in pulmonary fibrosis, here we investigated whether this pathway is also important in lung development.

From a structural standpoint, lung development is classified into five progressive periods designated the embryonic, pseudoglandular, canalicular, saccular, and alveolar stages (8). Lung organogenesis begins during the embryonic stage, when right and left buds form as an outpouching of the foregut (9). Conducting airway development occurs through continuous branching and growth of these buds during the following pseudoglandular stage. Subsequently, during the canalicular and saccular stages, mesenchymal and epithelial cells begin to differentiate, and alveolar sac septation commences (8). During the final stage of alveolarization, the acinar surface increases, and true alveoli are formed and are stabilized by epithelial cell–produced surfactant (8). An early and late phase of alveolarization can be differentiated spatially and morphologically in rodents (10). In the early phase, primary alveolar septa form in the central regions of the lung and are characterized initially by a double capillary network. This network subsequently matures into a single capillary bed (11), which occurs by 3 weeks after birth in rats (10). In contrast, primary septa in the late phase of alveolarization form in the peripheral subpleural regions of the lung without an initial double capillary network (12). The timing of completion of the late phase of alveolarization is less well established. Septation in the late phase is driven by α-smooth muscle actin–expressing fibroblasts, which proliferate and migrate in the peripheral lung and deposit key extracellular matrix proteins (9). These cells appear transiently in the developing peripheral lung alveolar septa during development (13) and can be referred to as peripheral septal fibroblasts (PSFBs) or alveolar myofibroblasts (14); we will refer to them as PSFBs. Impairments of the proliferation, migration, and/or matrix deposition of these cells have been implicated in the defective alveolarization that characterizes neonatal chronic lung disease, or bronchopulmonary dysplasia (BPD) (14, 15).

Here we report evidence that a loss of LPA–LPA_1 signaling impairs alveolar

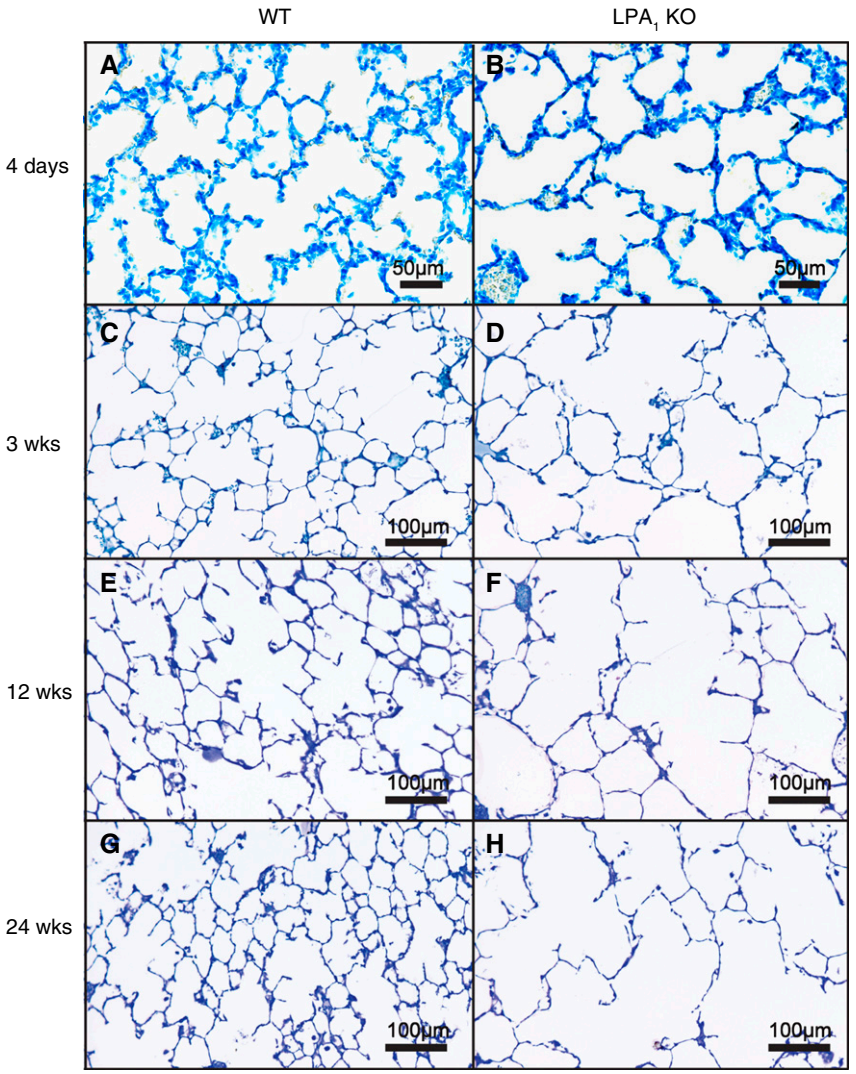

Figure 1. Airspace enlargement in lysophosphatidic acid receptor 1 (LPA_1) knock-out (KO) mice. LPA_1 KO mice exhibit enlarged and simplified distal airspaces throughout the alveolar stage of lung development. Representative toluidine blue–stained sections of fixed wild type (WT) and LPA_1 KO mouse lungs (*A* and *B*) at 4 days and (*C* and *D*) at 3 weeks, (*E* and *F*) 12 weeks, and (*G* and *H*) 24 weeks of age. Original magnification × 20. *Scale bars* represent 50 μm (*A* and *B*) or 100 μm (*C*–*H*).

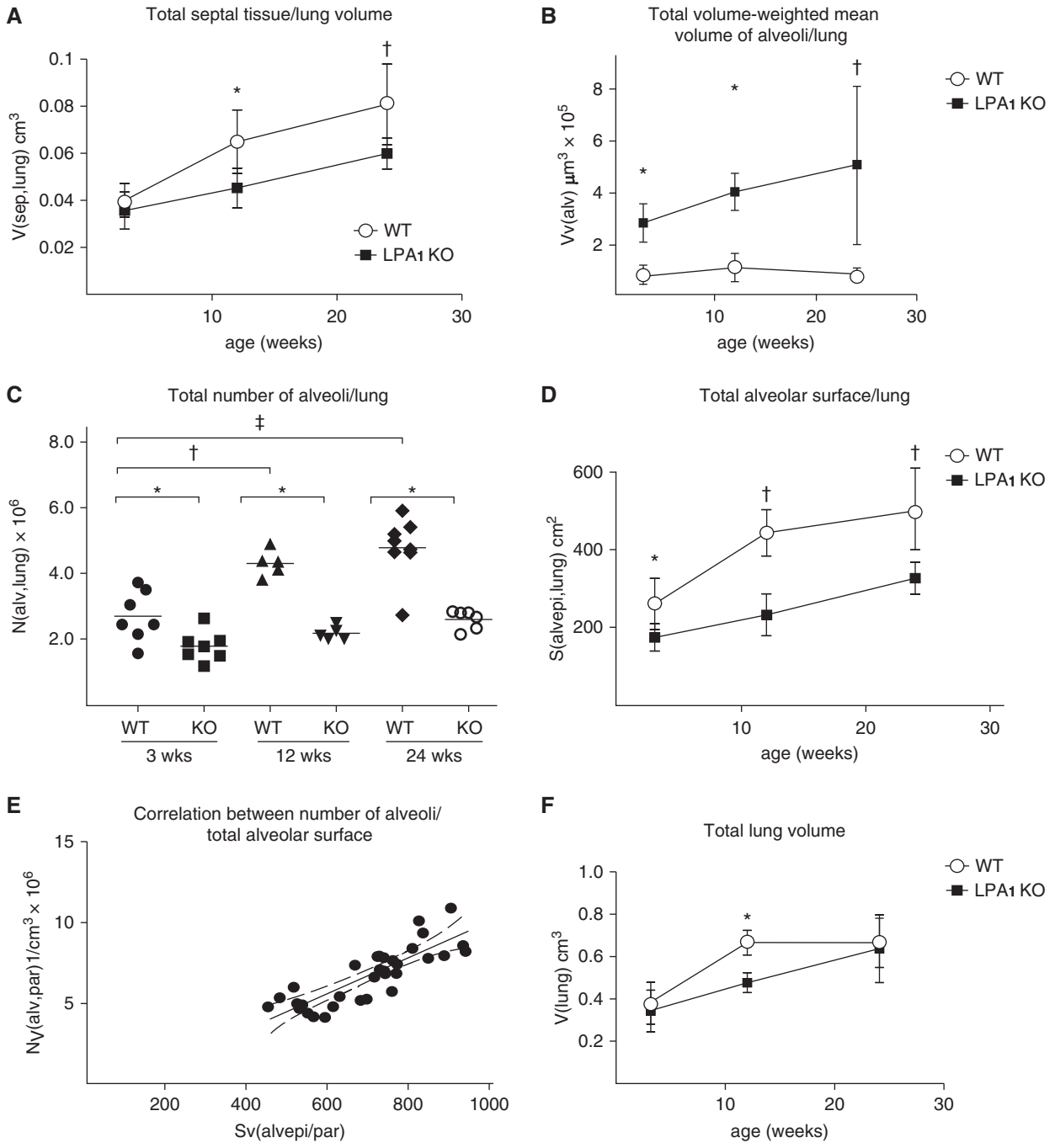

Figure 2. Quantitative assessment of airspace enlargement in LPA_1 KO mice by design-based stereology. (*A*) Total V(sep,lung) (cm^3) was significantly reduced in LPA_1 KO compared with WT mice at 12 weeks (*$P = 0.02$) and 24 weeks of age (†$P = 0.009$). (*B*) $V\nu$ (alv) (μm^3) was significantly increased in LPA_1 KO compared with WT mice at 3 weeks (*$P = 0.02$), 12 weeks (*$P = 0.02$), and 24 weeks of age (†$P = 0.03$). (*C*) Total N(alv,lung) were significantly decreased in LPA_1 KO compared with WT mice at 3, 12, and 24 weeks of age (*$P < 0.001$). Total numbers of alveoli in WT mice at 12 and 24 weeks were greater than in WT mice at 3 weeks of age by 38% and 44%, respectively (†$P = 0.00017$ and ‡$P = 0.00044$). (*D*) Total S(alvepi,lung) (cm^2) was significantly decreased in LPA_1 KO compared with WT mice at 3 (*$P = 0.01$), 12 (†$P < 0.001$) and 24 (†$P < 0.001$) weeks of age. (*E*) Correlation between N_V(alv,par) ($1/cm^3$) and total Sv(alvepi/par) in WT mice, considering mice assessed at 3, 12, and 24 weeks together. (*F*) Total V(lung) (cm^3) were significantly different between LPA_1 KO and WT mice only at 12 weeks of age, when they were lower in LPA_1 KO mice. *$P < 0.001$. For all comparisons, the following numbers of mice were examined: for mice at 3 weeks of age, seven WT and seven LPA_1 KO mice were examined; for mice at 12 weeks of age, five WT and five LPA_1 KO mice were examined; and for mice at 24 weeks of age, eight WT and seven LPA_1 KO mice were examined. In *A*, *B*, *D*, and *F*, data are presented as mean values ± standard deviation. In *C*, data are presented as individual animal values with means indicated by horizontal lines. N(alv,lung), numbers of alveoli per lung; N_V(alv,par), density of alveolar number within lung parenchyma; S(alvepi,lung), alveolar surface per lung; Sv(alvepi/par), density of alveolar surface area within lung parenchyma; V(sep,lung), septal tissue volume per lung; $V\nu$(alv), volume-weighted mean volume of alveoli.

septation. Quantitative assessment of lung architecture using design-based stereology demonstrated decreased numbers and total surface area of alveoli in LPA_1 knock-out (KO) mice, with increases in alveolar volumes, reminiscent of the alveolar dysplasia occurring in BPD (16). We found evidence that decreased elastin production and/or migration of LPA_1-deficient PSFBs may contribute to the observed impairment of alveolarization. The ability of LPA–LPA_1 signaling to direct fibroblast effector functions, which makes this pathway an attractive therapeutic target in the fibrotic pulmonary diseases that occur later in life, consequently may also be required for the normal lung development that occurs early in life. Some of the results of these studies have been reported previously in the form of an abstract (17).

Materials and Methods

Animals

LPA_1 KO and wild-type (WT) mice were bred from mice heterozygous for the LPA_1 mutant allele, as described previously (6), and the genotype of each mouse was determined before use in experiments by polymerase chain reaction (PCR) analysis of tail snip DNA. All mice were hybrids of the C57Bl/6 and 129Sv/J genetic backgrounds (kindly provided by Dr. Jerold Chun, Scripps Research Institute) (18). Experiments used sex-matched mice at age 4 days or 3, 12, or 24 weeks, maintained in specific pathogen-free environments, and were performed in accordance with U.S. National Institute of Health guidelines and protocols approved by the Massachusetts General Hospital Institutional Animal Care and Use Committee.

Lung Histological Staining

After the mice were killed, the lungs were fixed in a distended state. The P4 mouse pup lungs were fixed *in situ* as described previously (19). The older mouse lungs were fixed *in situ* after the vasculature was flushed via the right ventricle with ice-cold phosphate-buffered saline to remove blood cells. In both cases, a catheter was secured in the trachea, and the lungs were inflated to 20 cm H_2O pressure with 1.5% glutaraldehyde and 1.5% paraformaldehyde in 0.15 M HEPES buffer. For the quantitative morphometry, multiple plastic-embedded 1-μm sections of the entire mouse lung were stained with toluidine blue according to established protocols (20). For assessment of elastin morphology, 5-μm lung sections were stained with Hart's resorcin-fuchsin solution, without and with prior oxidation with potassium permanganate and clearing with oxalic acid, and counterstained with tartrazine as described previously (21). Bright-field microscopy was used to generate the lung images; the elastin images were constructed from a z-stack of lung images using extended depth-of-field focusing (22).

Quantitative Morphology by Design-Based Stereology

Stereological assessments were performed using recently published standards on quantitative morphology of the lung (23) (*see* online supplement for details).

Isolation of PSFBs

Fibroblasts and myofibroblasts, which are referred to together as PSFBs, were isolated from peripheral slices of 3-week-old LPA_1 KO and WT mouse lungs after enzymatic dissociation, as described (19). Previous work has characterized the identity of these cells (*see* online supplement for details).

RNA Isolation and Expression Analyses

Total RNA was extracted from snap-frozen lungs or primary PSFBs after each had been homogenized in TRIzol reagent (Thermo Fisher Scientific, Waltham, MA) using QIAGEN RNeasy kits (Quiagen, Hilden, Germany) according to the manufacturer's instructions. Total RNA from total lung was isolated after tissue homogenization and then extraction of RNA according to the manufacturer's instructions. Quantitative real-time PCR analysis was performed using an Mx4000 Multiplex Quantitative PCR System (Stratagene, La Jolla, CA) as described previously (24). Quantitative real-time PCR analysis primer sequences used are reported in Table E1 in the online supplement.

Western Blot Analyses

See online supplement.

PSFB Migration Assays

See online supplement.

Statistical Analyses

Statistical analyses were performed using a commercially available software package (GraphPad Prism 5.02; Software MacKiev, www.mackiev.com). Comparisons of parameters were assessed for statistical significance using a Student *t* test. Correlations between select parameters were assessed using a linear model of the data. A P value of <0.05 was considered statistically significant for all comparisons.

Results

Alveoli in LPA_1 KO Mice Are Increased in Size and Reduced in Number

Histological comparison of the lungs of WT and LPA_1 KO mice demonstrated

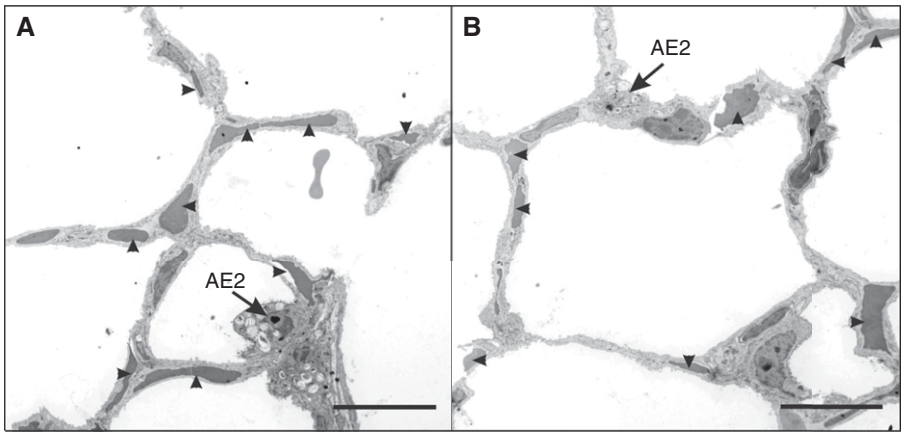

Figure 3. Early-phase alveolarization is completed by 3 weeks of age in WT and LPA_1 KO mice. Representative electron microscopy images of (*A*) LPA_1 KO and (*B*) WT mice indicate that mature single-layer capillary networks (*arrowheads*) are present in both genotypes. Four lungs per group. Original magnification × 2,200. *Scale bar* represents 10 μm. AE2, type 2 alveolar epithelial cells (*arrows*).

enlargement of the acinar airways in LPA_1 KO mice at all time points examined, from 4 days to 24 weeks of age (Figures 1A–1H). In P4 mouse lungs, secondary septation was already present, but these septa were fewer in LPA_1 KO lungs (Figures 1A and 1B); in older mice, decreased alveolarization seemed to be associated with enlargement of the distal airways in the KOs (Figures 1C–1H). We therefore performed design-based stereology to quantitatively compare lung tissues and alveolar volumes in WT and LPA_1 KO mice at 3, 12, and 24 weeks of age (23). Septal tissue volumes were reduced significantly in LPA_1 KO compared with WT mice at 12 and 24 weeks of age, by 30% and 26%, respectively (Figure 2A). Quantitation of alveolar volumes confirmed that they were increased in LPA_1 KO mice. Volume-weighted mean alveolar volumes were increased in LPA_1 KO compared with WT mice at 3, 12, and 24 weeks of age, by 3.5-, 3.5-, and 5.7-fold, respectively (Figure 2B). Moreover, the LPA_1 KO mice exhibited decreased alveolar numbers per lung at all time points examined, with reductions of 34%, 50%, and 46% at 3, 12, and 24 weeks, respectively (Figure 2C). Of note, our analyses of WT mice indicate that late alveolarization continues in mice during the period between 3 and 12 weeks of age (i.e., possibly well into adulthood). In WT

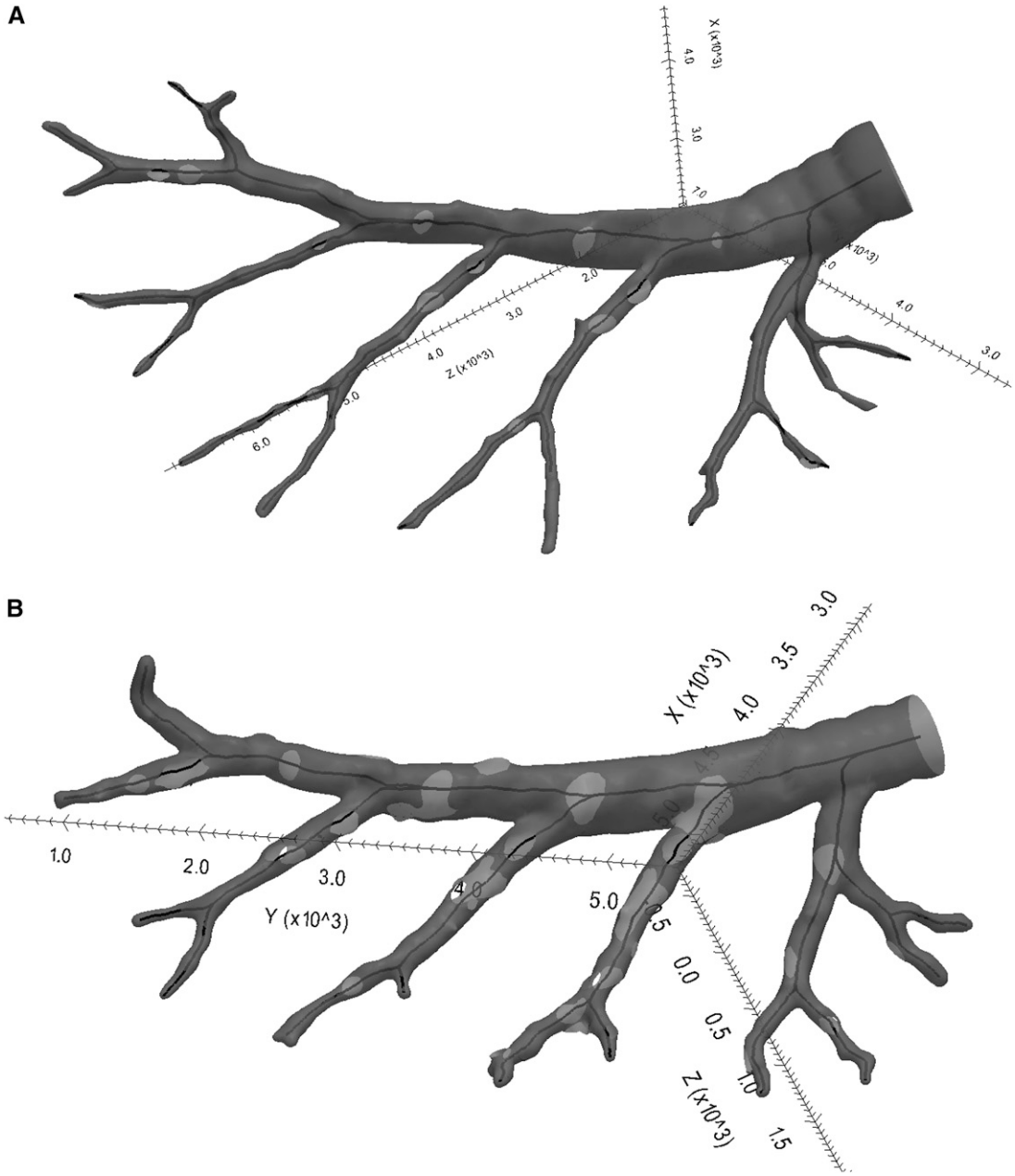

Figure 4. Branching morphogenesis is similar in WT and LPA_1 KO mice. Three-dimensional reconstructions of airways from scanning laser optical tomography of (*A*) WT and (*B*) LPA_1 KO mice at 3 weeks of age show similar branching morphology. Four lungs per group.

mice, the total number of alveoli per lung increased significantly by 38% between 3 and 12 weeks. Consistent with the reduced number and increased size of alveoli in LPA_1 KO mice, the total alveolar surface was significantly reduced in LPA_1-deficient lungs compared with WT mice at all time points investigated, by 33%, 48%, and 35% at 3, 12, and 24 weeks, respectively (Figure 2D). As an internal control for the consistency of our stereological assessments, the numbers of alveoli and the alveolar surface per lung were well correlated across mouse genotypes and time points examined (Figure 2E). To investigate the possibility that artifact-inducing overinflation of KO lungs during processing contributed to the increases in alveolar volumes determined to be present by designed-based stereology, we also determined total lung volumes in the two genotypes examined. At no time point examined did LPA_1 KO mice exhibit increased lung volumes compared with WT mice; total lung volumes were actually reduced by 29% in LPA_1 KO at 12 weeks of age (Figure 2F). These data suggest that the increases in alveolar volumes measured in the KO mice were not attributable to overinflation during processing. Our qualitative observation that secondary septation is decreased in P4 LPA_1 KO pups, coupled with our quantitative analyses indicating that distal airspace enlargement is already present in 3-week-old LPA_1 KO mice and that substantial alveolarization continues in the WT lung between 3 and 12 weeks of age, led us to hypothesize that the airspace enlargement that occurs in the LPA_1 KO animals is more likely a result of impaired formation of alveolar septa, rather than normal formation and subsequent increased loss.

Early and Late Alveolarization Are Impaired in LPA_1 KO Mice

As noted, the formation of alveolar septa in the early versus the late phases of the alveolarization stage of lung development can be distinguished by the nature of their capillary networks. Septal capillaries form initially as double-layered networks in the early phase of alveolarization, but resolve into single-layered networks in the late phase. Electron microscopy performed on the lungs of LPA_1 KO and WT mice at 3 weeks of age demonstrates the presence of single-layered capillary networks (Figure 3), suggesting that the early phase of

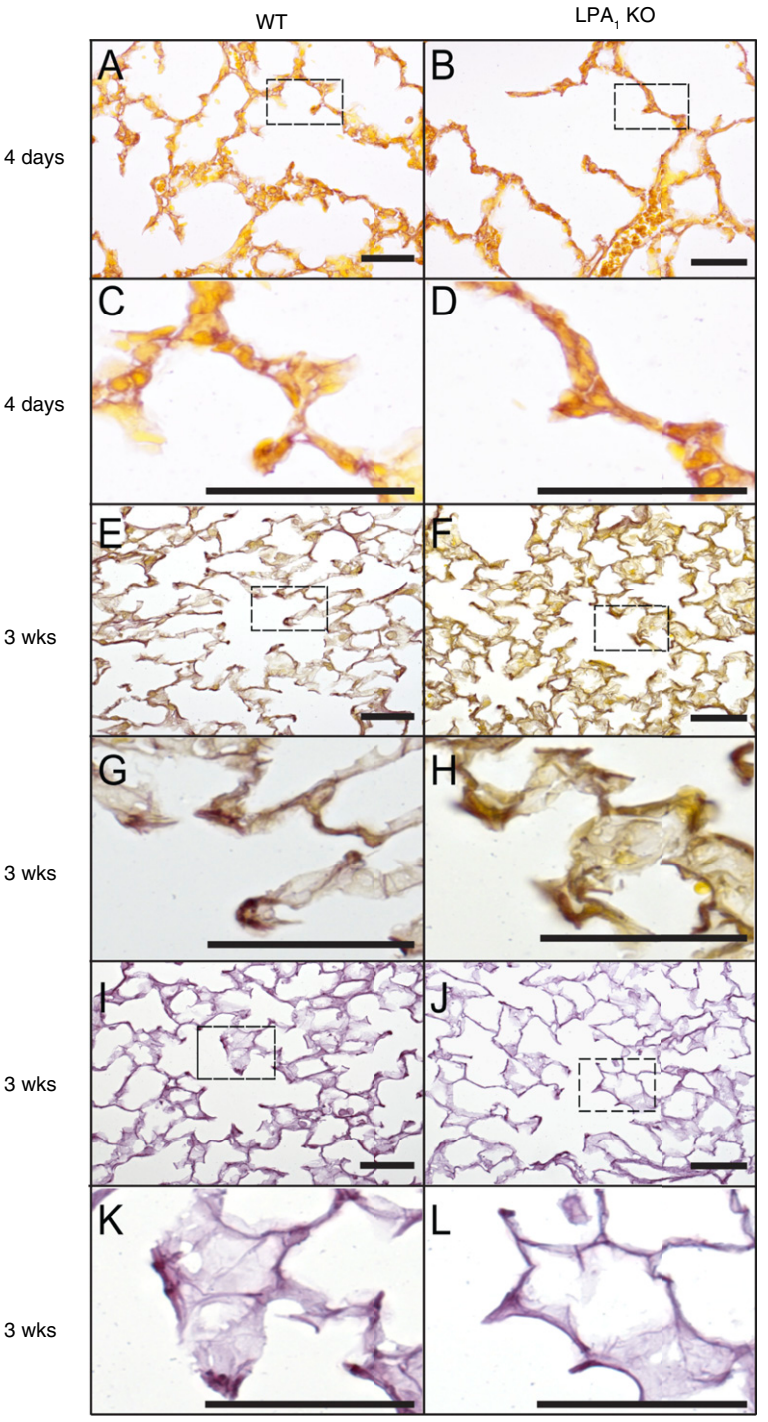

Figure 5. Disorganized and reduced septal elastic fibers in the lungs of LPA_1 KO mice. Hart's resorcin-fuchsin staining of lung sections without (*A–H*) and with (*I–L*) prior tissue oxidation, and tartrazine counterstaining. Original magnification × 20; *scale bars* are 100 μm. Comparison of stained nonoxidized sections of WT (*A*, *inset C*) and LPA_1 KO (*B*, *inset D*) mouse pup lungs at P4 demonstrates less organized, less condensed elastic fibers in the alveolar septa of the KO animals. Nonoxidized lung sections from 3-week-old WT (*E*, *inset G*) and LPA_1 KO (*F*, *inset H*) mice also demonstrate less organized, less condensed elastic fibers in the KOs, with areas in KO lungs in which the elastic fibers appear not to extend from the alveolar walls into the tips of the septa. Comparison of stained sections from 3-week-old WT (*I*, *inset K*) and LPA_1 KO (*J*, *inset L*) mice that were oxidized before staining to visualize all components of the elastic fiber system demonstrate overall decreased elastic fibers in the KO animals.

alveolarization has been completed by this time, as observed previously in other rodents (10). Our finding of decreased numbers of alveoli in LPA_1 KO mice at 3 weeks of age, coupled with our observation of decreased secondary septation in these mice at 4 days of age, suggests that early alveolarization is impaired in the absence of LPA_1 expression. The progressive reduction we observed in alveolar numbers in LPA_1 KO compared with WT mice from 3 to 12 weeks of age suggests that late alveolarization is impaired in the absence of LPA_1 expression as well.

Branching Morphogenesis Is Not Impaired in LPA_1 KO Mice

An impairment of branching morphogenesis could also decrease the number of alveoli that are formed during development, by decreasing the number of lung segments that are produced. To assess whether decreased branching morphogenesis contributes to the reduced number of alveoli that we observed in the LPA_1 KO mice, we qualitatively compared the branching pattern of the central conducting airways of LPA_1 KO mice with that of WT mice. As demonstrated in Figure 4, the branching patterns were similar between the genotypes, indicating that prenatal branching morphogenesis does not require LPA–LPA_1 signaling and that the observed reductions in alveolar numbers in LPA_1 KO mice are not attributable to defects in this process.

Alveolar Septal Elastogenesis Is Impaired in LPA_1 KO Mice

To further support our hypothesis that the airspace enlargement that we observed in LPA_1 KO mice is more likely caused by impaired formation of alveolar septa, rather than by normal formation and subsequent increased loss, we investigated whether (1) elastogenesis, a process central to the formation of alveolar septa, and/or (2) expression of mediators of alveolar septal loss, such as matrix metalloproteinases (MMPs) that cleave elastic fibers, are dysregulated in LPA_1 KO mice. Alveolarization requires tightly regulated fibroblast production of proteins, particularly of elastin, that become secreted and integrated into the functional extracellular matrix of developing septa (25). This leads to formation of an axial elastic fiber network, with preferential localization of elastic fibers in alveolar entrance rings, which contributes to alveologenesis and consequently influences alveolar number (26). Elastin cross-linking also regulates alveolar size, because its inhibition leads to the formation of enlarged distal air spaces in rodents (27, 28). We performed Hart's staining for elastic fibers in the lungs of LPA_1 KO and WT mice, which visualizes elaunin fibers and fully developed elastic fibers (FDEFs) when performed without prior oxidation of tissues, and all three components of the elastic fiber system, elaunin fibers, oxytalan fibers, and FDEFs, when performed with oxidation. Comparison of lung sections of WT and LPA_1 KO mice at P4 and 3 weeks of age that were not oxidized before staining demonstrated less organized, less condensed elastic fibers in the alveolar septa of the KO animals at both time points (Figures 5A–5H). Elastic fibers appeared not to extend from the alveolar walls into the tips of the septa in some areas of the lungs of 3-week-old LPA_1 KO mice. Comparison of lung sections of 3-week-old WT and LPA_1 KO mice that were oxidized before staining to visualize all components of the elastic fiber system demonstrated overall decreases in the number of elastic fibers present in the lungs of KO animals.

Reduced septal elastic fibers in LPA_1 KO mice could result from their decreased production, increased destruction, or both. To assess elastic fiber production, we measured tropoelastin mRNA expression in total lung homogenates. Tropoelastin mRNA was reduced significantly in LPA_1 KO versus WT mice at 3 weeks of age (Figure 6A), suggesting that decreased elastin production occurs in the absence of LPA_1 expression. To investigate whether LPA_1 deficiency could also increase elastic fiber destruction, we compared the expression of enzymes known to degrade these fibers, MMP-2, -7, -9, and -12 (29), and of an inhibitor of their activity, tissue inhibitor of metalloproteinase (TIMP)-3 (30), in LPA_1 KO and WT mice. Whereas MMP-2 and -7 mRNA expression was similar in whole lung homogenates of LPA_1 KO versus WT mice at 3 weeks of age, MMP-9 and -12 mRNA expression levels were actually significantly reduced, by 53% and 61%, respectively, in LPA_1 KO mice (Figures 6B–6E). TIMP-3 mRNA expression was also similar in LPA_1 KO versus WT lungs at 3 weeks of age (Figure 6F). Western blot analyses of α-elastin, MMP-9, and MMP-12 protein levels in the lungs of LPA_1 KO and WT mice at 3 weeks of age were consistent with mRNA expression results (Figure 6G). Levels of α-elastin protein appeared to be reduced in LPA_1 KO lungs. Differences in MMP-9 and MMP-12 protein levels were less apparent, but their expression was not increased in the KO animals. Taken together, these tropoelastin/α-elastin, MMP, and TIMP expression data suggest that impaired elastic fiber production, rather than increased degradation, is primarily responsible for the reduction in elastic fibers we observed in alveolar septa developing in the absence of LPA_1 expression.

Impaired Extracellular Matrix Production of LPA_1-Deficient PSFBs

As noted, fibroblasts and myofibroblasts residing in the peripheral lung play a critical role in regulating late alveolarization (9, 13, 14). Because our structural data indicated that this period of lung development was significantly affected by the absence of LPA_1, we compared the matrix protein expression pattern of these cells isolated from LPA_1 KO and WT pups, from ~1-mm-thick layers of the lung periphery that excludes large airways and vessels that we obtained with the aid of a dissecting microscope (19). As we have described previously, the fibroblasts that we isolated from the lung periphery of mouse pups were a mixture of α-smooth muscle actin–negative and –positive cells (19), suggesting that they were a mixture of fibroblasts and myofibroblasts that we refer to together as PSFBs. As demonstrated in Figure 7A, tropoelastin mRNA expression was reduced significantly by 42% in LPA_1-deficient versus WT PSFBs, consistent with the overall reduction in tropoelastin expression we observed in total lung homogenates of LPA_1 KO mice. In contrast, expression levels of procollagen $1\alpha_1$ and fibronectin mRNA by LPA_1-deficient PSFBs were not significantly different.

Impaired Migration of LPA_1-deficient PSFBs

We also compared the migration of PSFBs isolated from the lungs of LPA_1 KO and WT mice at 3 weeks of age. We noted previously that LPA is the predominant fibroblast chemoattractant induced in the lungs of adults with idiopathic pulmonary fibrosis and mice in the bleomycin model of pulmonary fibrosis, and that the migratory

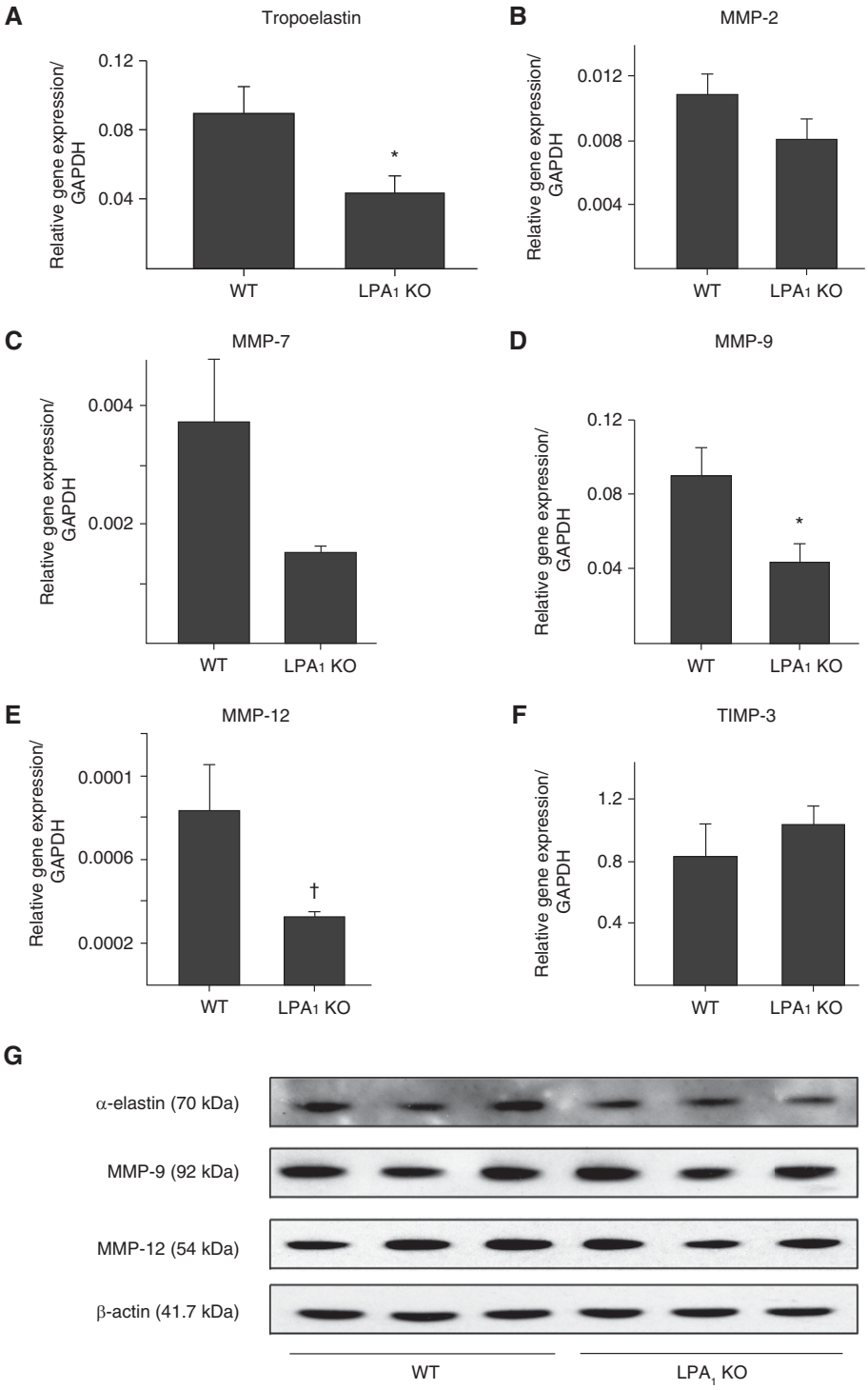

Figure 6. Reduced elastin and matrix metalloproteinase (MMP) production in the lungs of LPA_1 KO mice. (*A*) Tropoelastin mRNA expression was significantly reduced in total lung homogenates from LPA_1 KO compared with WT mice at 3 weeks of age (*$P < 0.03$); (*B*) MMP-2 and (*C*) MMP-7 mRNA expression was not significantly different between LPA_1 KO and WT mice at 3 weeks of age; (*D*) MMP-9 and (*E*) MMP-12 mRNA expression was significantly reduced in total lung homogenates from LPA_1 KO mice (*$P < 0.03$ and †$P = 0.04$); and (*F*) TIMP-3 mRNA expression was not significantly different. Data in *A* to *F* are presented as the mean expression of the gene of interest relative to GAPDH, ± SEM and have been combined from three independent experiments with three to six WT and three to four LPA_1 KO mice/experiment. (*G*) Western blotting suggests that levels of α-elastin protein are reduced in the lungs of LPA_1 KO compared with WT mice at 3 weeks of age. Differences in MMP-9 and MMP-12 protein levels were less apparent, but their expression was not increased in the KO animals. GAPDH, glyceraldehyde phosphate dehydrogenase; TIMP, tissue inhibitor of metalloproteinase.

responses of fibroblasts to LPA in pulmonary fibrosis are mediated specifically by LPA_1 (6), Similar to primary adult lung fibroblasts, LPA induced the migration of WT PSFBs, and this LPA-induced migration was almost completely abrogated in LPA_1-deficient cells, whereas the platelet derived growth factor-induced migration of these cells was preserved (Figure 7B). These data indicate that LPA-induced migration of PSFBs is also mediated primarily by LPA_1 rather than by other LPA receptors and suggest that LPA-induced PSFB migration would be largely eliminated in LPA_1 KO mice.

Altered MMP and TIMP Expression in LPA_1-deficient PSFBs

In addition to their roles in extracellular matrix remodeling, MMPs have been found to regulate the migration of cells, including fibroblasts. MMP-2 and MMP-9, for example, have been implicated in the migration and invasion of fibroblast-like synoviocytes in the pathogenesis of rheumatoid arthritis (31), and LPA signaling through LPA_1 has been shown to regulate MMP expression, including that of MMP-2 (32). We consequently compared MMP expression in PSFBs isolated from the lungs of LPA_1 KO and WT mice at 3 weeks of age. MMP-2, MMP-7, and MMP-9 mRNA expression levels were significantly reduced in LPA_1-deficient compared with WT PSFBs, by 62%, 28%, and 80%, respectively (Figure 7C). TIMP-3 mRNA expression levels were significantly increased by 1.7- fold in PSFBs from LPA_1-deficient versus WT mice (Figure 7C). These alterations in MMP and TIMP expression could reduce the ability of PSFBs to migrate through matrix in response to chemoattractants other than LPA, thus potentially causing a broader PSFB migration defect in LPA_1 KO mice and further contributing to impaired alveolar septation.

Discussion

We have shown that LPA signaling specifically through the LPA_1 receptor is required for normal lung development. Alveolarization but not branching morphogenesis was impaired in LPA_1-deficient mice, resulting in reduced numbers of alveoli that were increased in size in adult LPA_1 KO compared with WT mice. Our data suggest that this phenotype results from the impaired formation of alveolar septa during early- and late-phase alveolarization, rather than from the destruction of already formed septa. Our observation of significant increases in the numbers of alveoli present in WT mice between 3 and 12 weeks old also indicates that the late phase of alveolarization extends into adulthood in mice.

Lung development is orchestrated by the coordinated activities of multiple cell types. Septation in late alveolarization appears to depend particularly on the controlled migration and extracellular matrix production of PSFBs (9, 13, 14). With respect to mechanisms through which LPA–LPA_1 signaling may contribute to alveolarization, we found that several important functions of PSFBs, including migration and production of elastin, were impaired in the absence of LPA_1 expression. Of the extracellular matrix proteins, production and maturation of elastin appear to be central to alveolar septation (25). Reduced lung tropoelastin mRNA expression has also been associated with impaired alveolarization in Smad3-deficient mice (33). Impairment of elastin cross-linking in rats also led to impaired alveolarization with enlarged distal air spaces (28), similar to those we observed in the context of impaired elastin production in LPA_1 KO mice. We hypothesize that the impaired migration and elastin production of LPA_1-deficient PSFBs resulted in the reduced expression of elastin mRNA and protein we observed in lung homogenates of LPA_1 KO mice at 3 weeks of age, and the disorganized, discontinuous, and reduced elastic fiber network we observed in the alveolar septa of these mice at this time point, and earlier at P4.

Airspace enlargement developing in adult mice in both Smad3- and β6-integrin-subunit–deficient mice has been found to be associated with increased MMP-9 and/or -12 expression, producing a phenotype resembling the emphysema of adult human chronic obstructive pulmonary disease (33–35). Data from other mouse models, and from human studies, have implicated these two elastolytic MMPs, particularly MMP-12, in emphysema progression (29). In contrast to Smad3- and β6-deficient mice, however, lung expression levels of both MMP-9 and -12 were reduced in LPA_1 KO mice, further supporting our hypothesis that the phenotype of reduced alveolar numbers and increased alveolar volumes in LPA_1 KO mice results from the impaired formation of alveolar septa rather than from the destruction of already formed septa.

Although degradation of matrix proteins may be central to the role of some MMPs in destructive lung diseases such as emphysema (29), unanticipated phenotypes of multiple MMP KO mice have highlighted other MMP functions, including important roles in cell migration. MMPs have been found to be required for the establishment of chemoattractant gradients (36) and for enabling cells including fibroblasts to migrate through matrix in response to these gradients (37). In the context of these and other functions, individual deficiencies in several MMPs have been found to decrease rather than increase lung matrix protein deposition in models of pulmonary fibrosis, including MMP-3, -7, and -8 (36, 38, 39). We observed that the expression of multiple MMPs, including MMP-2, -7 and -9, by PSFBs was significantly reduced in LPA_1 KO mice, possibly reducing their ability to migrate through matrix during the formation of alveolar septa. Reduced production of multiple MMPs by LPA_1-deficient PSFBs consequently could also contribute to impaired alveolarization in LPA_1 KO, by impairing migration of these cells.

Impaired alveolarization has become the hallmark of BPD associated with infant prematurity. Advances in the medical therapy of premature infants in recent decades has greatly improved their survival and has significantly changed the clinical and pathological features of BPD associated with premature birth, as reviewed recently (15). As it was described initially, BPD was characterized by evidence of severe lung injury, including inflammation, protein-rich lung edema, extensive airway epithelial metaplasia, peribronchial fibrosis, and marked airway and pulmonary vascular smooth muscle hypertrophy (40). In contrast, advances in neonatal care, including the use of antenatal steroids, surfactant replacement therapy, and lung protective strategies of ventilation, have mitigated lung injury in premature infants and have transformed the pulmonary phenotype of BPD to one dominated by the disruption of alveologenesis (16). The development of therapies to mitigate or treat impaired alveologenesis in premature infants will require a better understanding of the mechanisms and mediators of

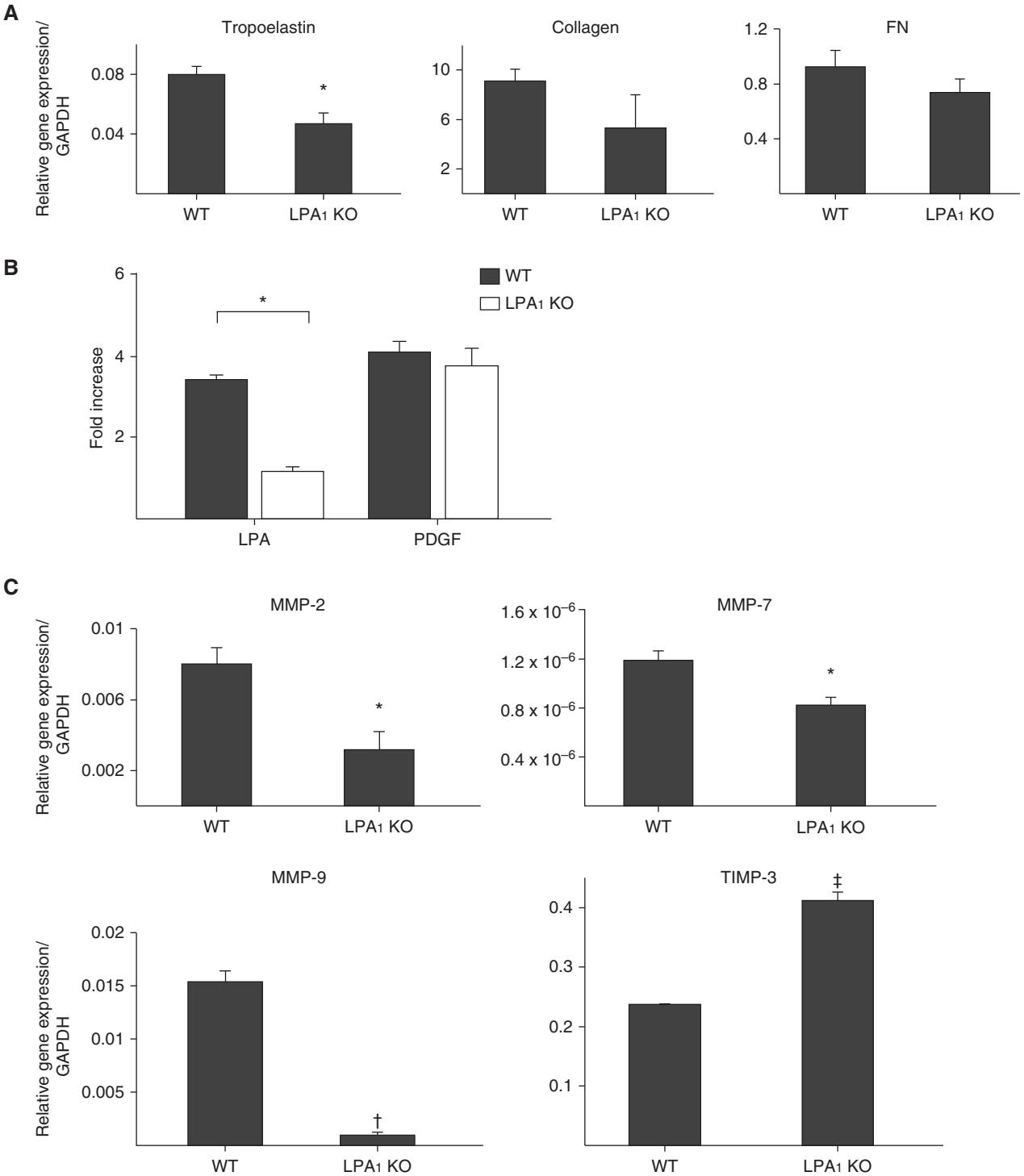

Figure 7. Impaired tropoelastin production and migration of LPA_1–deficient peripheral septal fibroblasts (PSFBs). (*A*) PSFBs isolated from LPA_1 KO mice at 3 weeks of age demonstrated significantly reduced tropoelastin expression compared with PSFBs isolated from WT mice of the same age (*$P = 0.02$). Collagen and fibronectin (FN) expression were not significantly different between LPA_1 KO and WT PSFBs. Data are presented as mean expression of the gene of interest relative to GAPDH, ± SEM. (*B*) PSFBs isolated from LPA_1 KO mice at 3 weeks of age demonstrated significantly reduced migration induced by LPA (10 μM) compared with PSFBs isolated from WT mice of the same age (*$P = 0.00006$) but had similar migration induced by platelet-derived growth factor (PDGF)-BB (10 ng/ml). Data are presented as mean fold-increase of migration induced by the chemoattractant compared with migration induced by media alone, ± SEM. (*C*) PSFBs isolated from LPA_1 KO mice at 3 weeks of age demonstrated significantly reduced MMP-2 (*$P = 0.02$), MMP-7 (*$P = 0.02$), and MMP-9 (†$P = 0.0002$) expression and significantly increased TIMP-3 expression (‡$P = 0.00025$) compared with PSFBs isolated from WT mice of the same age. Data are presented as mean expression of the gene of interest relative to GAPDH, ± SEM.

alveolar septation; the results presented in our study suggest that the LPA signaling specifically through LPA_1 is required for this process.

In contrast to the physiological role we identified for LPA–LPA_1 signaling in lung development, this pathway has been implicated in the pathogenesis of multiple lung diseases, including asthma, acute lung injury, and pulmonary fibrosis (41). We have previously implicated LPA–LPA_1 signaling in the development of fibrosis in multiple organs, including the lung (6, 42), the skin (43), and the peritoneum (44), whereas others have implicated this pathway in renal and hepatic fibrosis (45, 46). In the development of organ fibrosis, we have found that LPA–LPA_1 signaling promotes fibroblast recruitment, proliferation, activation, and persistence (5, 6, 44). Here we have found evidence that LPA–LPA_1 signaling promotes PSFB migration and matrix production. Hence, some of the same LPA_1-mediated fibroblast functions whose loss protects LPA_1 KO mice from pathological fibrosis appear to contribute to the failure of physiological alveolarization that we now observe in these mice.

Lastly, we observed that increases in the numbers of alveoli continued to occur well into adulthood in WT mice. Stereological analysis revealed a significant increase in alveolar number occurred in the WT mouse lung between 3 and 12 weeks, and a trend toward a further increase from 12 to 24 weeks. During this period, the number of alveoli nearly doubled. Late alveolarization has been reported to continue postnatally through Day 36 in mice (12) and Day 60 in rats (47). Similar observations of alveolarization continuing into adulthood have been made in rabbits, monkeys, and, most recently, humans (48–50). Alveolar size and number were assessed noninvasively by helium-3 magnetic resonance in children and adolescents from 7 to 21 years of age, and the alveolar number was estimated to increase nearly twofold across this age range (50). Continued alveolarization during childhood, adolescence, and even early adulthood raises concerns that lung injury in these periods of life can adversely affect pulmonary development, but it also raises the possibility that ongoing lung septation may permit recovery of lost tissue and pulmonary function during this time (50).

Conclusions

In summary, we have implicated the LPA–LPA_1 pathway in lung development by showing that interruption of LPA–LPA_1 signaling leads to a spontaneous impairment of early and late alveolarization. The onset of this phenotype during the alveolarization stage of lung development, its association with reduced PSFB elastin production, and its occurrence in the absence of increased lung MMP expression suggest that it results from impaired alveolar septation as the lung develops, rather than from increased septal destruction as occurs in the emphysema of chronic obstructive pulmonary disease. In contrast to our prior studies in pulmonary fibrosis, which have indicated that antagonizing LPA–LPA_1 signaling may be able to mitigate that pathology (5, 6), the current study suggests that augmenting LPA–LPA_1 signaling may have the potential to contribute to future strategies to stimulate alveolar septation when that may be beneficial. ■

Author disclosures are available with the text of this article at www.atsjournals.org.

References

1. Yung YC, Stoddard NC, Chun J. LPA receptor signaling: pharmacology, physiology, and pathophysiology. *J Lipid Res* 2014;55:1192–1214.
2. Sheng X, Yung YC, Chen A, Chun J. Lysophosphatidic acid signalling in development. *Development* 2015;142:1390–1395.
3. Yung YC, Stoddard NC, Mirendil H, Chun J. Lysophosphatidic acid signaling in the nervous system. *Neuron* 2015;85:669–682.
4. Kihara Y, Maceyka M, Spiegel S, Chun J. Lysophospholipid receptor nomenclature review: IUPHAR Review 8. *Br J Pharmacol* 2014;171: 3575–3594.
5. Funke M, Zhao Z, Xu Y, Chun J, Tager AM. The lysophosphatidic acid receptor LPA_1 promotes epithelial cell apoptosis after lung injury. *Am J Respir Cell Mol Biol* 2012;46:355–364.
6. Tager AM, LaCamera P, Shea BS, Campanella GS, Selman M, Zhao Z, Polosukhin V, Wain J, Karimi-Shah BA, Kim ND, *et al*. The lysophosphatidic acid receptor LPA_1 links pulmonary fibrosis to lung injury by mediating fibroblast recruitment and vascular leak. *Nat Med* 2008;14:45–54.
7. Selman M, Pardo A, Kaminski N. Idiopathic pulmonary fibrosis: aberrant recapitulation of developmental programs? *PLoS Med* 2008;5:e62.
8. Smith LJ, McKay KO, van Asperen PP, Selvadurai H, Fitzgerald DA. Normal development of the lung and premature birth. *Paediatr Respir Rev* 2010;11:135–142.
9. Schittny JC, Burri P. Development and growth of the lung. In: Fishman AP, Elias JA, Fishman JA, Grippi MA, Senior RM, Pack AI, editors. Fishman's pulmonary diseases and disorders, 4 ed. New York, NY: McGraw-Hill Medical; 2008. pp. 91–114.
10. Burri PH. Structural aspects of postnatal lung development - alveolar formation and growth. *Biol Neonate* 2006;89:313–322.
11. Amy RW, Bowes D, Burri PH, Haines J, Thurlbeck WM. Postnatal growth of the mouse lung. *J Anat* 1977;124:131–151.
12. Mund SI, Stampanoni M, Schittny JC. Developmental alveolarization of the mouse lung. *Dev Dyn* 2008;237:2108–2116.
13. Yamada M, Kurihara H, Kinoshita K, Sakai T. Temporal expression of α-smooth muscle actin and drebrin in septal interstitial cells during alveolar maturation. *J Histochem Cytochem* 2005;53:735–744.
14. Kim N, Vu TH. Parabronchial smooth muscle cells and alveolar myofibroblasts in lung development. *Birth Defects Res C Embryo Today* 2006;78:80–89.
15. Hilgendorff A, Reiss I, Ehrhardt H, Eickelberg O, Alvira CM. Chronic lung disease in the preterm infant. Lessons learned from animal models. *Am J Respir Cell Mol Biol* 2014;50:233–245.
16. Margraf LR, Tomashefski JF Jr, Bruce MC, Dahms BB. Morphometric analysis of the lung in bronchopulmonary dysplasia. *Am Rev Respir Dis* 1991;143:391–400.
17. Funke M, Knudsen L, Matthieu S, Fontaine B, Chun J, Ochs M, Tager AM. The role of the lysophosphatidic acid (LPA) receptor 1 in developmental alveolarization [abstract]. *ERJ* 2013;42(Suppl 57):3331.
18. Contos JJ, Fukushima N, Weiner JA, Kaushal D, Chun J. Requirement for the LPA1 lysophosphatidic acid receptor gene in normal suckling behavior. *Proc Natl Acad Sci USA* 2000;97:13384–13389.
19. Bachiller PR, Cornog KH, Kato R, Buys ES, Roberts JD Jr. Soluble guanylate cyclase modulates alveolarization in the newborn lung. *Am J Physiol Lung Cell Mol Physiol* 2013;305:L569–L581.
20. Mühlfeld C, Knudsen L, Ochs M. Stereology and morphometry of lung tissue. *Methods Mol Biol* 2013;931:367–390.
21. Pieretti AC, Ahmed AM, Roberts JD Jr, Kelleher CM. A novel *in vitro* model to study alveologenesis. *Am J Respir Cell Mol Biol* 2014;50:459–469.
22. Forster B, Van De Ville D, Berent J, Sage D, Unser M. Complex wavelets for extended depth-of-field: a new method for the fusion of multichannel microscopy images. *Microsc Res Tech* 2004;65:33–42.
23. Hsia CC, Hyde DM, Ochs M, Weibel ER; ATS/ERS Joint Task Force on Quantitative Assessment of Lung Structure. An official research policy statement of the American Thoracic Society/European

Respiratory Society: standards for quantitative assessment of lung structure. *Am J Respir Crit Care Med* 2010;181:394–418.
24. Means TK, Hayashi F, Smith KD, Aderem A, Luster AD. The Toll-like receptor 5 stimulus bacterial flagellin induces maturation and chemokine production in human dendritic cells. *J Immunol* 2003;170: 5165–5175.
25. Bourbon J, Boucherat O, Chailley-Heu B, Delacourt C. Control mechanisms of lung alveolar development and their disorders in bronchopulmonary dysplasia. *Pediatr Res* 2005;57:38R–46R.
26. Ochs M, Nyengaard JR, Jung A, Knudsen L, Voigt M, Wahlers T, Richter J, Gundersen HJ. The number of alveoli in the human lung. *Am J Respir Crit Care Med* 2004;169:120–124.
27. McGowan SE. Extracellular matrix and the regulation of lung development and repair. *FASEB J* 1992;6:2895–2904.
28. O'Dell BL, Kilburn KH, McKenzie WN, Thurston RJ. The lung of the copper-deficient rat. A model for developmental pulmonary emphysema. *Am J Pathol* 1978;91:413–432.
29. Houghton AM. Matrix metalloproteinases in destructive lung disease. *Matrix Biol* 2015;44-46:167–174.
30. Basu R, Lee J, Morton JS, Takawale A, Fan D, Kandalam V, Wang X, Davidge ST, Kassiri Z. TIMP3 is the primary TIMP to regulate agonist-induced vascular remodelling and hypertension. *Cardiovasc Res* 2013;98:360–371.
31. Li G, Zhang Y, Qian Y, Zhang H, Guo S, Sunagawa M, Hisamitsu T, Liu Y. Interleukin-17A promotes rheumatoid arthritis synoviocytes migration and invasion under hypoxia by increasing MMP2 and MMP9 expression through NF-κB/HIF-1α pathway. *Mol Immunol* 2013;53: 227–236.
32. Kato K, Fukui R, Okabe K, Tanabe E, Kitayoshi M, Fukushima N, Tsujiuchi T. Constitutively active lysophosphatidic acid receptor-1 enhances the induction of matrix metalloproteinase-2. *Biochem Biophys Res Commun* 2012;417:790–793.
33. Chen H, Sun J, Buckley S, Chen C, Warburton D, Wang XF, Shi W. Abnormal mouse lung alveolarization caused by Smad3 deficiency is a developmental antecedent of centrilobular emphysema. *Am J Physiol Lung Cell Mol Physiol* 2005;288:L683–L691.
34. Bonniaud P, Kolb M, Galt T, Robertson J, Robbins C, Stampfli M, Lavery C, Margetts PJ, Roberts AB, Gauldie J. Smad3 null mice develop airspace enlargement and are resistant to TGF-β-mediated pulmonary fibrosis. *J Immunol* 2004;173:2099–2108.
35. Morris DG, Huang X, Kaminski N, Wang Y, Shapiro SD, Dolganov G, Glick A, Sheppard D. Loss of integrin $\alpha_v\beta_6$-mediated TGF-β activation causes Mmp12-dependent emphysema. *Nature* 2003;422:169–173.
36. Li Q, Park PW, Wilson CL, Parks WC. Matrilysin shedding of syndecan-1 regulates chemokine mobilization and transepithelial efflux of neutrophils in acute lung injury. *Cell* 2002;111:635–646.
37. Rowe RG, Keena D, Sabeh F, Willis AL, Weiss SJ. Pulmonary fibroblasts mobilize the membrane-tethered matrix metalloprotease, MT1-MMP, to destructively remodel and invade interstitial type I collagen barriers. *Am J Physiol Lung Cell Mol Physiol* 2011;301: L683–L692.
38. Yamashita CM, Dolgonos L, Zemans RL, Young SK, Robertson J, Briones N, Suzuki T, Campbell MN, Gauldie J, Radisky DC, *et al*. Matrix metalloproteinase 3 is a mediator of pulmonary fibrosis. *Am J Pathol* 2011;179:1733–1745.
39. Craig VJ, Quintero PA, Fyfe SE, Patel AS, Knolle MD, Kobzik L, Owen CA. Profibrotic activities for matrix metalloproteinase-8 during bleomycin-mediated lung injury. *J Immunol* 2013;190: 4283–4296.
40. Northway WH Jr, Rosan RC, Porter DY. Pulmonary disease following respirator therapy of hyaline-membrane disease. Bronchopulmonary dysplasia. *N Engl J Med* 1967;276:357–368.
41. Zhao Y, Natarajan V. Lysophosphatidic acid (LPA) and its receptors: role in airway inflammation and remodeling. *Biochim Biophys Acta* 2013;1831:86–92.
42. Montesi SB, Mathai SK, Brenner LN, Gorshkova IA, Berdyshev EV, Tager AM, Shea BS. Docosatetraenoyl LPA is elevated in exhaled breath condensate in idiopathic pulmonary fibrosis. *BMC Pulm Med* 2014;14:5.
43. Castelino FV, Seiders J, Bain G, Brooks SF, King CD, Swaney JS, Lorrain DS, Chun J, Luster AD, Tager AM. Amelioration of dermal fibrosis by genetic deletion or pharmacologic antagonism of lysophosphatidic acid receptor 1 in a mouse model of scleroderma. *Arthritis Rheum* 2011;63:1405–1415.
44. Sakai N, Chun J, Duffield JS, Wada T, Luster AD, Tager AM. LPA1-induced cytoskeleton reorganization drives fibrosis through CTGF-dependent fibroblast proliferation. *FASEB J* 2013;27: 1830–1846.
45. Pradère JP, Gonzalez J, Klein J, Valet P, Grès S, Salant D, Bascands JL, Saulnier-Blache JS, Schanstra JP. Lysophosphatidic acid and renal fibrosis. *Biochim Biophys Acta* 2008;1781: 582–587.
46. Watanabe N, Ikeda H, Nakamura K, Ohkawa R, Kume Y, Tomiya T, Tejima K, Nishikawa T, Arai M, Yanase M, *et al*. Plasma lysophosphatidic acid level and serum autotaxin activity are increased in liver injury in rats in relation to its severity. *Life Sci* 2007; 81:1009–1015.
47. Tschanz SA, Salm LA, Roth-Kleiner M, Barré SF, Burri PH, Schittny JC. Rat lungs show a biphasic formation of new alveoli during postnatal development. *J Appl Physiol (1985)* 2014;117:89–95.
48. Kovar J, Sly PD, Willet KE. Postnatal alveolar development of the rabbit. *J Appl Physiol (1985)* 2002;93:629–635.
49. Hyde DM, Blozis SA, Avdalovic MV, Putney LF, Dettorre R, Quesenberry NJ, Singh P, Tyler NK. Alveoli increase in number but not size from birth to adulthood in rhesus monkeys. *Am J Physiol Lung Cell Mol Physiol* 2007;293:L570–L579.
50. Narayanan M, Owers-Bradley J, Beardsmore CS, Mada M, Ball I, Garipov R, Panesar KS, Kuehni CE, Spycher BD, Williams SE, *et al*. Alveolarization continues during childhood and adolescence: new evidence from helium-3 magnetic resonance. *Am J Respir Crit Care Med* 2012;185:186–191.